Cancer Chemother Pharmacol (2007) 59:733–742
DOI 10.1007/s00280-006-0327-1

ORIGINAL ARTICLE

The range of optimal concentration and mechanisms of paclitaxel in radio-enhancement in gastrointestinal cancer cell lines

Yuji Toiyama · Yasuhiro Inoue · Junichiro Hiro · Eiki Ojima · Hideki Watanabe · Youhei Narita · Atuko Hosono · Chikao Miki · Masato Kusunoki

Received: 17 May 2006 / Accepted: 10 August 2006 / Published online: 7 September 2006

Abstract
Aim This study was performed to investigate the range of optimal concentration and mechanisms of paclitaxel (PXL) radio-enhancement in gastrointestinal cancer cell lines HT29 and MKN45.
Methods Cell growth inhibition by PXL pretreatment at various concentrations (0–10 μM) followed by irradiation was investigated using a modified MTT assay. To investigate the mechanisms of the observed radio-enhancement, flow cytometry was conducted to define the cell cycle distributions. Furthermore, the alterations in expression of a DNA repair molecule [excision repair cross-complementation group1 (ERCC1)] and an angiogenesis factor [vascular endothelial growth factor (VEGF)] induced by PXL were investigated.
Results Cytotoxic concentrations of PXL (0.1–10 μM) that cause accumulation of cells in the G2/M phase have strong radio-enhancing effects and inhibit total cell growth. The maximal non-cytotoxic concentration of PXL (0.01 μM) also had a radio-enhancing effect. The expression of the genes of ERCC1 and VEGF induced by radiation was suppressed by PXL pretreatment. The protein secretion of VEGF induced by radiation was suppressed at cytotoxic doses of PXL, and the induced protein secretion of ERCC1 was also suppressed even at maximal non-cytotoxic doses of PXL.
Conclusion The range of optimal concentration for PXL pretreatment was 0.01–0.1 μM in these cells. Two major mechanisms of radio-enhancement are suggested: (1) PXL induces G2/M arrest leading to increased DNA damage after radiation, which results in mitotic death, and (2) PXL suppresses the expression of radiation-induced DNA repair molecules and angiogenesis factors, resulting in inhibition of cell growth and cell death.

Keywords ERCC1 · G2/M arrest · Paclitaxel · Radio-enhancement · VEGF

Y. Toiyama · Y. Inoue · J. Hiro · E. Ojima · H. Watanabe · Y. Narita · A. Hosono · C. Miki · M. Kusunoki (✉)
Department of Gastrointestinal and Pediatric Surgery, Division of Reparative Medicine, Institute of Life Sciences, Mie University Graduate School of Medicine, 2-174 Edobashi, Tsu, Mie 514-8507, Japan
e-mail: kusunoki@clin.medic.mie-u.ac.jp

Introduction

The combination of conventional chemotherapy with radiation is now used for definitive adjuvant therapy in the majority of cancer patients. Randomized trials have shown that combination treatment improves survival compared with radiation alone in the treatment of locally advanced cancers of the head and neck, lung, esophagus, stomach, pancreas and rectum. Despite these resounding clinical successes, the mechanisms by which conventional chemotherapeutic agents produce radio-sensitization remain largely unknown.

Paclitaxel (PXL) is one of the most promising anticancer drugs developed in the last two decades [1]. It has been shown that PXL blocks the progression of cells at the G2/M boundary of the cell cycle by inhibiting the dynamic reorganization of the microtubule network required for spindle formation

during cell mitosis [2, 3]. The radio-sensitizing effects of PXL have been investigated extensively on the rationale that G2/M is the most radio-sensitive phase of the cell cycle [4, 5]. In most of these combination studies, a significant radiation-potentiating effect of PXL was found only after a dose that produced both a block in G2/M phase and a high level of cell death in the clinical setting. This could result in damage to normal tissue.

However, the increased cell radio-sensitivity with exposure to PXL is evident at very low drug concentrations, below those required for the cytotoxic effects or G2/M arrest. Furthermore, G2/M arrest does not result in PXL radio-sensitization in all cell types and sensitivity persists well after the relatively brief period of G2/M synchronization, suggesting that other cellular factors may be involved in this process [6]. Recent studies [7, 8] have investigated new combination schedules with radiation and low, sub-therapeutic PXL doses that did not result in cell cycle perturbation. These studies aimed to obtain information on: (a) the best synergistic effect as a result of the optimal combination of cell line characteristics, growth phase, drug concentration and scheduling; and (b) the cellular mechanism of action of PXL-mediated radio-sensitization, in terms of cytokinetic alterations, interference with post-irradiation DNA repair, apoptosis and reoxygenation [9, 10].

The present study aimed to establish the range of optimal concentration of PXL in relation to two main issues [(1) cell growth inhibition with PXL pretreatment followed by radiation, and (2) the radio-enhancing effects of PXL pretreatment], using clinically relevant doses of PXL, with an aim to clarify the mechanisms of radio-enhancement induced by PXL pretreatment at various doses in gastrointestinal cancer cell lines.

Materials and methods

Cell culture

Human adenocarcinoma cell lines HT29 and MKN45 were obtained from the Cell Resource Center for Biomedical Research, Institute of Development, Aging and Cancer, Tohoku University. These cell lines were grown in RPMI1640 (Sigma-Aldrich, St Louis, MO, USA), supplemented with fetal bovine serum [FBS; 10% (v/v); Gibco BRL, Tokyo, Japan], glutamine (2 mM), penicillin (1,000 U/ml) streptomycin (100 μg/ml) at 37°C in a 5% CO_2 incubator.

Anticancer agents

PXL was obtained from Sigma-Aldrich, reconstituted in distilled water at appropriate concentrations, and stored at −20°C until use.

Experimental concept

We used clinical concentrations of PXL as much as possible. PXL doses were chosen based on plasma concentrations obtained during clinical use, cited in the drug information for TAXOL INJECTION (Bristol Myers Squibb, Tokyo, Japan). This information indicated that the plasma concentration of PXL reaches 1–10 μg/ml (1–10 μM) after injection and 0.05–0.1 μg/ml (0.05–0.1 μM) at 24 h after drip infusion of 105–270 mg/m^2. Irradiation was carried out at fixed doses of 0 and 2.5 Gy. All irradiation treatments were performed on a CLINAC 2100C X-ray system (Varian Oncology Services, USA) at 4 MV using 40 mm solid water phantom with a dose rate of 217 cGy/min.

Drug concentration, irradiation and drug administration schedules

As mentioned above, we adopted clinically relevant concentrations of PXL in this study. Although we should ideally consider the doubling time of each cell line before deciding the drug exposure time, we chose to use an exposure time of 24 h for experimental simplicity. The final concentration ranged from 0.001 to 10 μM.

To test the cytotoxicity of PXL, each cell line was treated in the exponential growth phase for 24 h with various concentrations of PXL. After discarding the media containing the drug and replacing it with fresh media, the cytotoxicity was evaluated using a modified MTT assay ([2-(2-methoxy-4-nitrophenyl)-3-(4-nitrophenyl)-5-(2,4-disulfophenyl)-2H-tetrazolium, monosodium salt] (WST-8) colorimetric assay).

For irradiation experiments, cells of each cell line were first treated with clinical concentrations of PXL for 24 h, except for the no-PXL controls. After removing the drug and ?lling the wells with fresh medium, irradiation was carried out at 2.5 Gy. Irradiated cells were incubated for 0, 24 or 48 h, and the cell growth inhibition was evaluated using a modified MTT assay. The drug-exposure and irradiation schedules are summarized in Table 1.

Modified MTT assay

The cytotoxicity was evaluated using a WST-8 colorimetric assay. WST-8 is a modification of the MTT assay, which was applied to estimation of cellular via-

Table 1 (a) Schematic representation of drug exposure schedule. (b) Schematic representation of drug followed by radiation exposure schedule

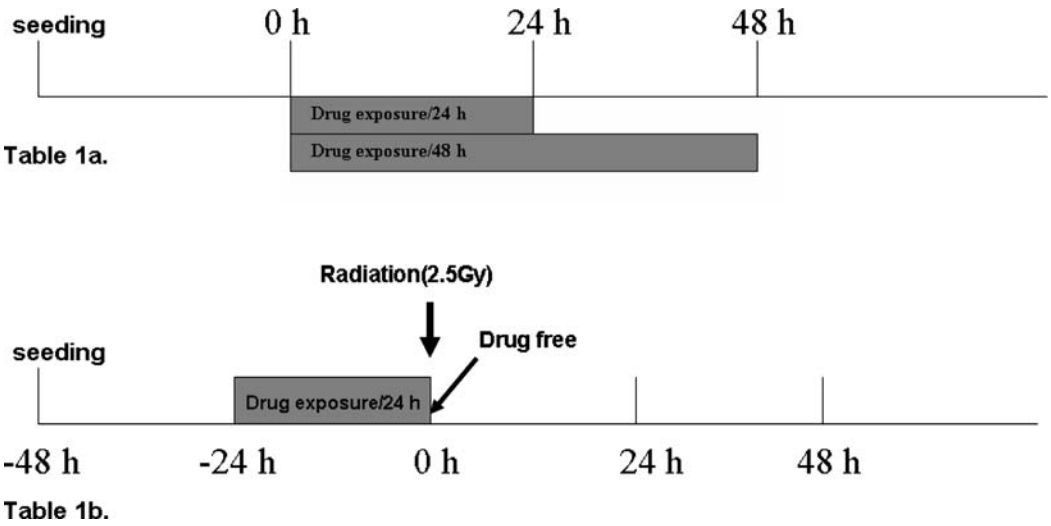

bility using a commercially available kit (cell counting kit, Dojindo Laboratories, Japan).

Cell cycle analysis by flow cytometry

Each cell line was treated with various concentrations of PXL for 24 h. The cell cycle distribution was determined by flow cytometric analysis as described previously [34].

RNA extraction and semiquantitive RT-PCR analysis

RNA was isolated from each cell line using an RNeasy™ Mini Kit (QIAGEN). Oligo(dT)-primed cDNA was prepared from this RNA (2 μg) by reverse transcription using an Omniscript RT kit (QIAGEN). RT-PCR was performed using the specific primers described in Table 2. Optimal cycling parameters, in the linear range of amplification, consisted of 30 s denaturation at 94°C, 30 s annealing at 60°C, and 1 min elongation at 72°C, and 23–28 cycles were performed for the selected gene. A control PCR was also performed for β-actin, which served as a standard for sample normalization for 25 cycles. Amplified products were separated electrophoretically, visualized, and photographed under UV light after ethidium bromide staining.

Table 2 Primer sets for reverse transcription-PCR

VEGF	Sense	5′-CTTGCCTTGCTGCTCTACCT-3′
	Antisense	5′-ATGATTCTGCCCTCCTCCTT-3′
ERCC1	Sense	5′-ACAGAGCCTCGCCTTTGC-3′
	Antisense	5′-GCGGCGATATCATCATCC-3′
B-actine	Sense	5′-ACAGAGCCTCGCCTTTGC-3′
	Antisense	5′-GCGGCGATATCATCATCC-3′

Protein extraction and western blot analysis

HT29 and MKN45 cells were homogenized in lysis buffer (Tris-buffered saline, pH 7.5, containing 1% Triton X-100) for 5 min on ice. After spinning at 15,000 rpm for 15 min at 4°C, supernatants were collected and frozen at −20°C until use. The protein concentration was measured by the BCA protein assay (Pierce, Rockford, IL, USA). Lysates containing 10 μg total protein were mixed with an equal volume of 2 × Lammeli's loading buffer, containing 2ME, and heated at 100°C for 5 min. Samples were electrophoretically separated on 12.5% gradient polyacrylamide gels containing 0.1% SDS at 25 mA for 2 h, followed by semi-dry transfer to an Immun-Blot PVDF membrane (Bio-Rad, Hercules, CA, USA) at 12 V for 2 h. The membranes were blocked for 1 h at room temperature using 5% skimmed milk in Tris-buffered saline, pH 7.5, supplemented with 0.1% Tween 20 (TBS-T). The blots were then incubated with mouse monoclonal anti- excision repair cross-complementation group1 (ERCC1) (Santa Cruz Biotechnology) antibody at a 1:100 dilution, and mouse monoclonal anti-actin (clone C4) antibody (ICN Biomedicals, Aurora, OH, USA) at a 1:3,000 dilution in 5% skimmed milk in TBS-T overnight at 4°C. After being washed three times in TBS-T, the blots were incubated with alkaline phosphatase-conjugated goat anti-mouse IgG (Promega, Madison, WI, USA) at a 1:1,000 dilution in 5% skimmed milk in TBS-T for 1 h at room temperature. Following treatment with

an enhanced chemiluminescence detection solution, the blots were exposed to X-ray film for autoradiographic visualization of the bands.

Conditioned medium (CM) harvesting

CM was harvested from supernatant which was treated according to the protocol and stored at −20°C until use.

ELISA

The concentration of vascular endothelial growth factor (VEGF) in the CM was measured using a commercially available ELISA kit (Immunoassay Kit Human VEGF; Biosource International, Camarillo, CA, USA) according to the manufacturer's protocol.

Statistical analysis

The results are expressed as the means ± SD. The Mann–Whitney *U* test was used for comparisons among unpaired groups. $P < 0.05$ was considered statistically significant.

Results

Growth inhibition of HT29 and MKN45 cells by PXL

We first evaluated the dose-dependent effect of PXL on cell viability. The cytotoxic effects of PXL were assessed at 24 h after drug exposure, using a modified MTT assay. PXL at a concentration of 0.1 μM (used clinically for drip infusion) and 1–10 μM (used clinically for injection) inhibited HT29 and MKN45 cell growth in a dose-dependent manner (Fig. 1). We defined PXL concentrations of less than or equal to 0.01 μM as non-cytotoxic and more than or equal to 0.1 μM as cytotoxic. Therefore, the maximal non-cytotoxic dose of PXL for each cell line was 0.01 μM.

Cell growth inhibition by PXL pretreatment and radiation

HT29 and MKN45 cells were treated with PXL (0.001–10 μM) for 24 h. After removing the drug from the wells and filling the wells with fresh medium, cells were irradiated at a dose of 0 or 2.5 Gy. Growth inhibition was measured by a modified MTT assay. The results are shown in Fig. 2a, b. PXL pretreatment followed by radiation-inhibited growth in both cell lines in a time- and dose-dependent manner. This effect was shown to be greater at cytotoxic doses than at non-cytotoxic doses of PXL pretreatment, for both 24 and 48 h after treatment ($P < 0.05$). Furthermore, PXL pretreatment with maximal non-cytotoxic doses also significantly inhibited cell growth ($P < 0.05$), but this inhibition was lower than that with PXL pretreatment at cytotoxic doses.

Radio-enhancing effect of PXL pretreatment

To measure the radio-enhancing effect of PXL on HT29 and MKN45 cells, we calculated the growth ratio of 24 h viable cells per 0 h viable cells and 48 h viable cells per 0 h viable cells. Inhibition of growth rate signifies a radio-enhancing effect. Fig. 3a and b show that the growth rate in both cell lines following radiation was significantly lower after treatment with PXL at 0.01–1 μM than at 0–0.001 μM for 24 and 48 h ($P < 0.05$). Furthermore, PXL 0.01–1 μM

Cell lines	PXL concentration	Cell viability±SD (%)/control	P value	
HT29	0.001 μM	101.72±5.85		Non Cytotoxic Dose
	0.01 μM	96.04±5.11		
	0.1 μM	70.26±2.54	<0.05 *	Cytotoxic Dose
	1 μM	67.76±3.40	<0.05 *	
	10 μM	65.25±3.50	<0.05 *	
MKN45	0.001 μM	107.88±6.26		Non Cytotoxic Dose
	0.01 μM	101.21±3.16		
	0.1 μM	83.29±1.95	<0.05 *	Cytotoxic Dose
	1 μM	72.02±4.57	<0.05 *	
	10 μM	68.55±2.61	<0.05 *	

Fig. 1 PXL cytotoxicity in MKN45 (**a**) and HT29 (**b**) cells. Cells were treated with different concentrations (0.001, 0.01, 0.1, 1 or 10 μM) of PXL for 24 h, and cell growth was determined using a modified MTT assay. Results are expressed as percentage cell growth relative to untreated control cells. The data represent the mean ± SD of eight experiments

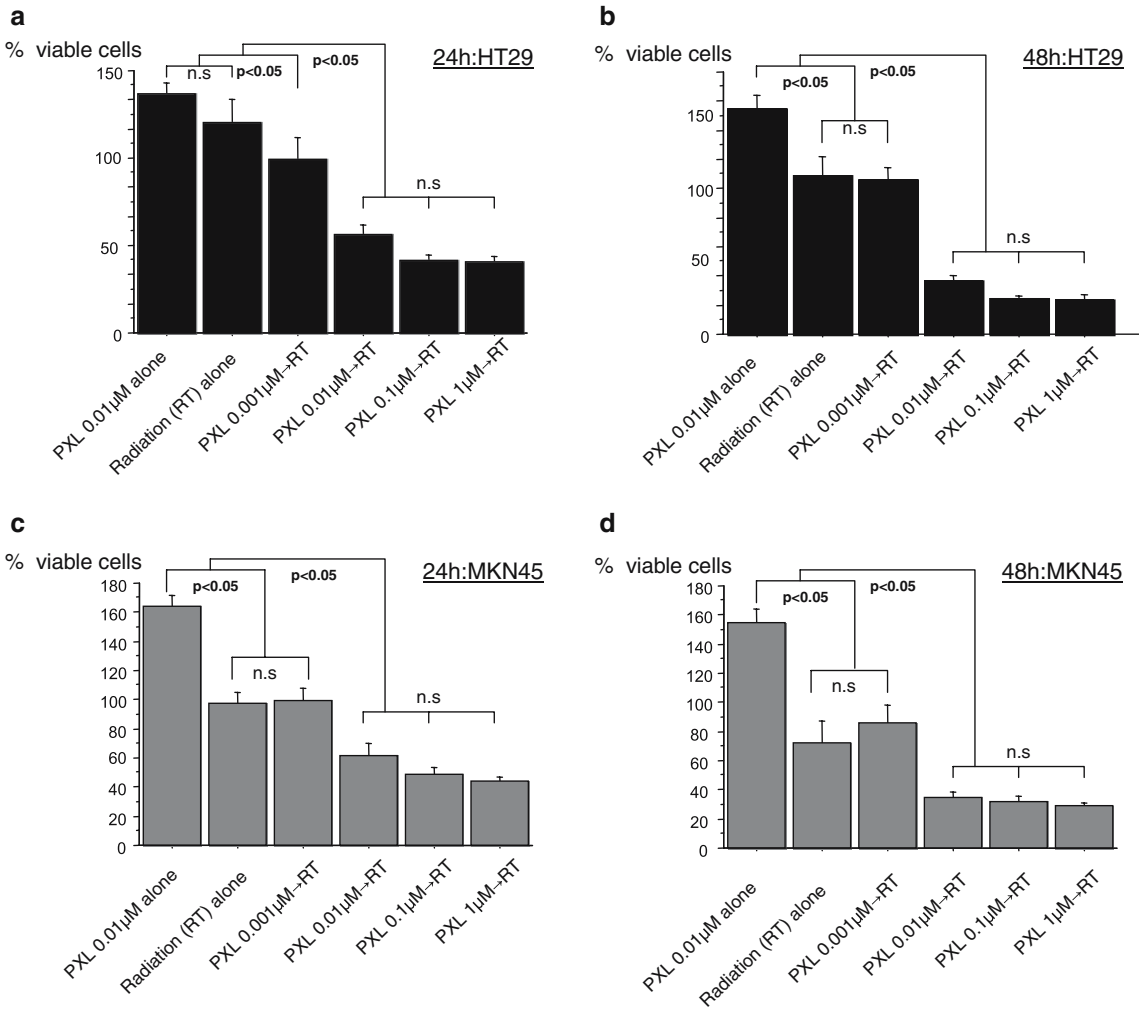

Fig. 2 Growth inhibition of MKN45 (**a**) and HT29 (**b**) cells with PXL pretreatment followed by radiation. Cells were treated with PXL (0.001, 0.01, 0.1, or 1 μM for 24 h) followed by 2.5 Gy radiation, and cell growth at 0, 24 and 48 h after radiation was determined using a modified MTT assay. Results are expressed as percentage cell growth relative to PXL (0.001μM) followed by irradiation. The data represent the mean ± SD of eight experiments

pretreatment had a similar effect on growth rate both 24 and 48 h.

Cell cycle distribution in HT29 and MKN45 cells following PXL treatment

Cell cycle distribution has long been known to contribute to radio-sensitivity. The S phase is the most radioresistant, and the G2/M phase is usually the most radiosensitive. We investigated cell cycle distribution in HT29 and MKN45 cells after PXL treatment for 24 h. There were no significant differences in the cell cycle distribution of either cell line treated with non-cytotoxic doses of PXL for 24 h, versus no treatment. However, in MKN45 cells, there was significant accumulation in the G2/M phase after 24 h exposure to cytotoxic doses of PXL, in a dose-dependent manner (Fig. 4a). In comparison, cell distribution analysis in HT29 cells after PXL exposure for 24 h at all cytotoxic doses revealed 90% or more of cells in the G2/M phase, but in a non dose-dependent manner (Fig. 4b).

The changes in VEGF secretion in CM following PXL treatment

VEGF protein secretion in CM increased in a time-dependent manner. However, VEGF secretion under PXL exposure at cytotoxic doses (0.1–10 μM) was significantly suppressed compared to that under PXL exposure at non-cytotoxic doses, for both 24 and 48 h (*1, *2, $P < 0.05$, NS not significant). The inhibitory effect on VEGF secretion of PXL treatment at 0.1 μM was the same as for PXL treatment at 1 and 10 μM (Fig. 5a, b).

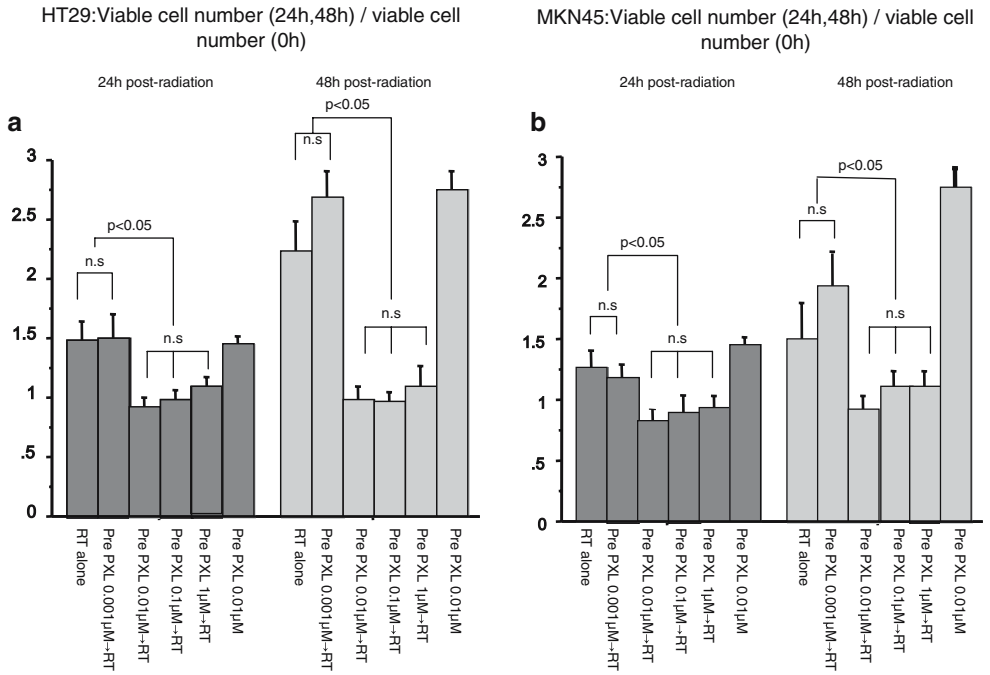

Fig. 3 Radio-enhancement effects in MKN45 (**a**) and HT29 (**b**) cells after PXL pretreatment. We calculated the ratios of 24 h, 48 h viable cell numbers per 0 h viable cell numbers after PXL pretreatment (0, 0.001, 0.01, 0.1 or 1 μM for 24 h) followed by irradiation. Inhibition of growth rate signifies a radio-enhancing effect. The data represent the mean ± SD of eight experiments

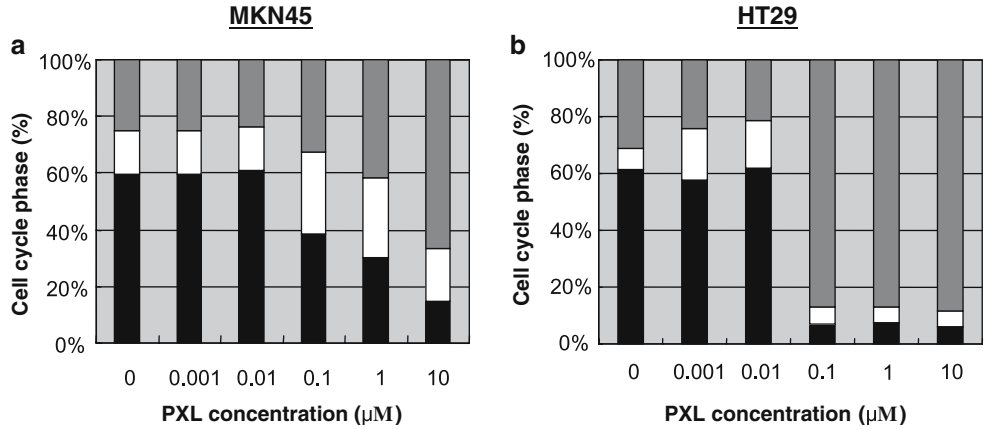

Fig. 4 Effects of PXL exposure for 24 h on the cell cycle distribution of MKN45 (**a**) and HT29 (**b**) cells. Each cell line was treated with PXL (0.001, 0.01, 0.1, 1, or 10 μM) for 24 h. The cells were then harvested and the cell cycle distributions were analyzed by flow cytometry. The results from three separate experiments were averaged, and the percentages of cells in the G1, S and G2/M phases are shown in a *vertical stacked bar* graph format. The *black bars* represent G1, the *white bars* are S, and the *gray bars* are G2/M

The effect of PXL pretreatment followed by radiation on VEGF expression, measured by RT-PCR and ELISA

VEGF gene expression was induced by radiation without PXL pretreatment. However, in cells, which were pretreated with PXL, VEGF gene expression was significantly inhibited at 24 h after radiation, relative to radiation without PXL treatment (Fig. 5c). VEGF protein secretion in CM was gradually increased in a time-dependent fashion by radiation alone. However, pretreatment with PXL at cytotoxic doses significantly inhibited VEGF protein secretion induced at 24 and 48 h after radiation (*1, *2,$P < 0.05$) (Fig. 5d).

Effect of PXL pretreatment followed by radiation on ERCC1 expression, measured by RT-PCR and western blotting

ERCC1 gene expression was induced by radiation without PXL pretreatment. However, in cells pretreated with

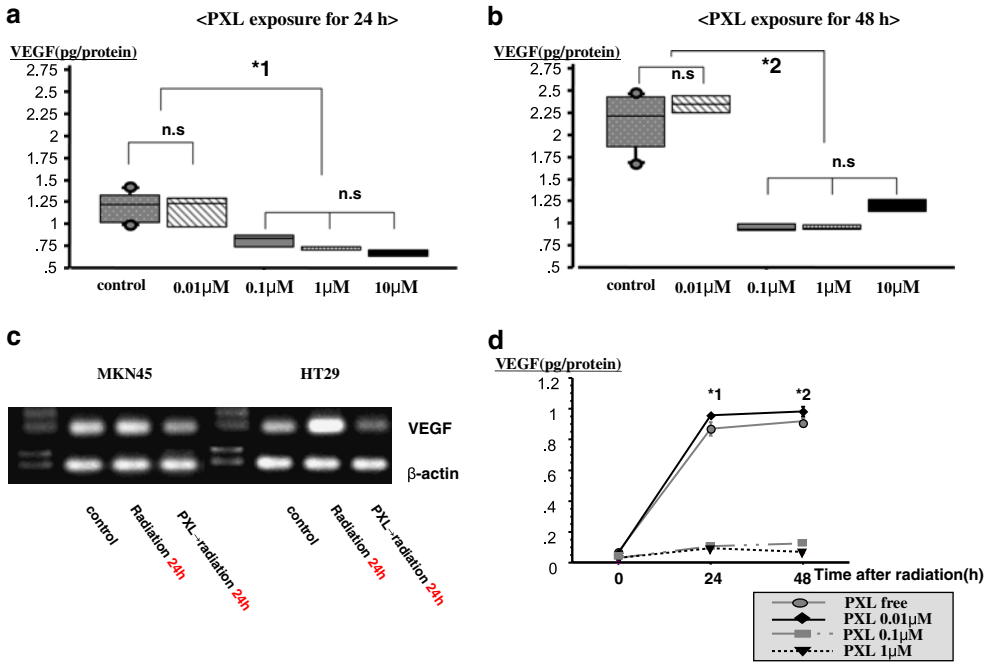

Fig. 5 Effects of PXL treatment or PXL pretreatment followed by irradiation on VEGF expression. The cells were incubated in various concentrations of PXL control, 0.01, 0.1, 1, 10 μM for 24 h (**a**) and 48 h (**b**). VEGF protein expression levels in conditioning medium (CM) were evaluated at 24 and 48 h using an ELISA system. The data indicate the mean ± SD of the experiments carried out in triplicate; (**c**) VEGF gene expression under various conditions was evaluated by semi-quantitative RT-PCR. A control PCR was also carried out for β-actin, which served as a standard for sample normalization; (**d**) cells were pretreated with PXL (0, 0.01, 0.1 or 1 μM for 24 h) followed by irradiation. VEGF protein secretion levels in CM were evaluated by ELISA at 0, 24 and 48 h after radiation. The data represent the mean ± SD of three experiments

PXL followed by radiation, ERCC1 gene expression was significantly inhibited versus radiation alone (Fig. 6a). Furthermore, PXL pretreatment at cytotoxic doses significantly inhibited ERCC1 protein expression induced at 0, 24 and 48 h after radiation. Interestingly, PXL pretreatment even at maximal non-cytotoxic doses significantly inhibited ERCC1 protein expression at 0, 24 and 48 h after radiation (Fig. 6b).

Discussion

In this study, we attempted to establish the range of optimal concentration for PXL pretreatment to obtain a radio-enhancing effect and cell growth inhibition in two human adenocarcinoma cell lines, HT29 and MKN45. This was based on previous studies indicating that PXL pretreatment for 24 h prior to radiation [7, 8] leads to a radio-sensitizing effect. Since the present study was focused on the sequential effect of PXL pretreatment on radiation, we removed PXL from wells before radiation treatment.

The cell growth inhibition induced by PXL pretreatment followed by radiation was shown to be strongly dependent on PXL dose. In both cell lines, cytotoxic PXL pretreatment followed by radiation significantly inhibited cell growth compared to non-cytotoxic doses. However, among the cytotoxic doses of PXL pretreatment, there were no differences in cell growth inhibition. Thus, radio-enhancement was shown to be strongly induced by PXL pretreatment in a dose-dependent manner, but only in terms of this cytotoxic versus non-cytotoxic dose difference.

To understand the influence of PXL pretreatment on the cell cycle, we performed flow-cytometric analysis. The results revealed that cytotoxic doses of PXL caused accumulation of cells in the G2/M phase in both cell lines. These results suggest that sufficient concentrations of PXL cause freezing of microtubules and G2/M phase arrest, this phase being the most radiosensitive phase of the cell cycle. Interestingly, maximal non-cytotoxic doses of PXL also have the potential to inhibit cell growth and induce radio-enhancement. Since flow-cytometric analysis showed that there were no significant differences in the cell cycle distribution at these concentrations compared to control, other cellular mechanisms of action must be involved in non-cytotoxic PXL-mediated radio-enhancement.

To understand the radio-enhancing effect of pretreatment with non-cytotoxic doses of PXL, we searched for

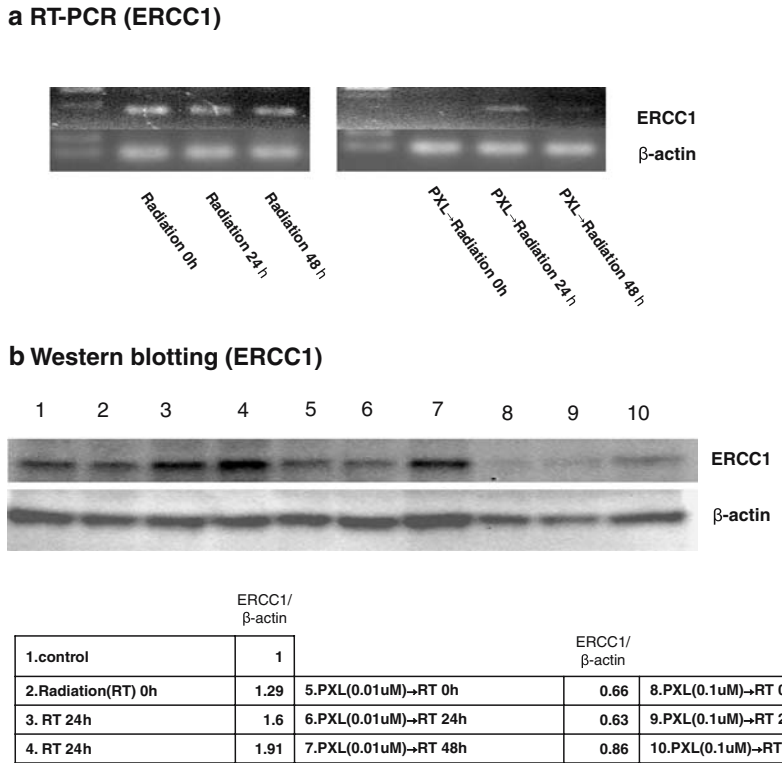

	ERCC1/β-actin		ERCC1/β-actin		ERCC1/β-actin
1.control	1				
2.Radiation(RT) 0h	1.29	5.PXL(0.01uM)→RT 0h	0.66	8.PXL(0.1uM)→RT 0h	0.37
3. RT 24h	1.6	6.PXL(0.01uM)→RT 24h	0.63	9.PXL(0.1uM)→RT 24h	0.8
4. RT 24h	1.91	7.PXL(0.01uM)→RT 48h	0.86	10.PXL(0.1uM)→RT 48h	0.58

Fig. 6 Effect of PXL pretreatment and irradiation on ERCC1 expression. **a** ERCC1 gene expression under various conditions was evaluated by semi-quantitative RT-PCR. A control PCR was also carried out for β-actin, which served as a standard for sample normalization; **b** cells were pretreated with PXL (0, 0.01 or 0.1 μM for 24 h) followed by irradiation. ERCC1 protein levels were evaluated by western blotting at 0, 24 and 48 h after radiation. The films were scanned and the relative quantities of the protein bands were analyzed by densitometry using CS Analyzer version 2.0 (ATTO Corporation, Japan). The experiments were carried out in triplicate

other possible contributory factors. Although various intrinsic and extrinsic factors affecting radio-sensitization, including hypoxia and angiogenesis [11], DNA double-strand breakage repair [12], and p53 gene status [13], have been reported, we focused on angiogenesis and DNA repair which may be potential mechanisms of the radio-enhancement observed in this study.

VEGF is the most potent and specific growth factor for endothelial cell activation [14]. Evidence for the importance of VEGF-induced angiogenesis in tumor growth was demonstrated by experiments using neutralizing antibodies or a dominant-negative soluble receptor to inhibit VEGF action and the growth of primary and metastatic tumors [15]. Direct up-regulation of VEGF after irradiation in various cancer cell lines has been reported [16], and some studies targeting the VEGF/VEGFR signaling pathway in conjunction with irradiation have been conducted. Gorski et al. [16] found that antibodies to VEGF, when combined with ionizing radiation in vitro, resulted in increased endothelial cell death without affecting tumor cells. In contrast, VEGF has been shown to reduce apoptosis after irradiation in human leukemia cells and in human and murine mammary adenocarcinoma cells [17, 18]. Furthermore, Hovinga et al. showed that high basal VEGF secretion was associated with greater resistance to irradiation in glioblastoma in vitro [19].

In this study, VEGF protein secretion was significantly downregulated by PXL exposure at cytotoxic doses. Furthermore, direct upregulation of VEGF protein after radiation was also significantly inhibited by cytotoxic doses of PXL. However, at non-cytotoxic doses, this phenomenon was not observed. Since PXL pretreatment at cytotoxic doses enhanced the effects of radiation and inhibited cell growth significantly, we speculate that one of the mechanisms in PXL enhancement of radiation effects is a decrease in VEGF secretion.

Next, the nucleotide excision repair pathway is one of the most important pathways that guards the integrity of the genome, removing a wide variety of DNA lesions including interstrand cross-links caused by cisplatin (CDDP) or radiation [20, 21]. Removal of these adducts from genomic DNA is mediated by a complex interaction of various proteins [22, 23]. A critical step in this

process is the interaction of the product of the *ERCC1* gene with the products of the Xeroderma Pigmentosum Group A (*XPA)* and group F (*XPF)* genes [24]. Previous reports have demonstrated increased *ERCC1* mRNA expression as an indicator for non-response to neoadjuvant CDDP-based chemotherapy for gastric cancer [25], colon cancer [26] and non-small cell lung cancer [27]. Recent study has also shown that decreased *ERCC1* mRNA expression is a predictor for response to neoadjuvant chemoradiotherapy for esophageal cancer [28]. Furthermore, experimental studies have demonstrated that increased ERCC1 levels are associated with removal of cisplatin-induced strand adducts and relative cisplatin resistance [29]. In addition, ERCC1-defective knockout mice are highly sensitive to DNA cross-linking agents [30]. ERCC1 is also associated with radiation-induced DNA damage, although this mechanism is still poorly understood [31, 32].

We have also demonstrated that radiation activated the DNA repair gene *ERCC1* using RT-PCR and Western blotting. Interestingly, PXL pretreatment inhibits ERCC1 gene expression even after radiation. Furthermore, Western blotting analysis shows that non-cytotoxic, as well as cytotoxic; doses of PXL inhibit ERCC1 protein upregulation at 0, 24 and 48 h after radiation. Yacoub et al. previously showed that the MEK inhibitor PD90859 blocked the induction of ERCC1 and ERCC1 by radiation, and cell death from radiation was maximal when PD90859 was added prior to radiation [33]. It is therefore conceivable that PXL pretreatment decreases expression of ERCC1 even after radiation, and might prevent the cells from undergoing DNA repair, resulting in radio-sensitization, even if non-cytotoxic doses of PXL are used.

In conclusion, the range of optimal concentration for PXL pretreatment was 0.01–0.1 μM, in the light of two main evaluations comprising the cell growth inhibition with PXL pretreatment, and the radio-enhancing effects of PXL resulting from this inhibition and other factors. In other words, two major mechanisms of tumor radio-sensitization are suggested: (1) PXL induces G2M arrest, this being the most radio-sensitive phase of the cell cycle and (2) PXL pretreatment suppresses the radiation-induced expression of VEGF and ERCC1, leading to greater DNA damage after radiation and resulting in the cell growth inhibition.

References

1. Rowinsky EK, Donehower RC (1995) Paclitaxel (taxol). N Engl J Med 332:1004–1014
2. Horwitz SB (1992) Mechanism of action of taxol. Trends Pharmacol Sci 13:134–136
3. Schiff PB, Horwitz SB (1980) Taxol stabilizes microtubules in mouse fibroblast cells. Proc Natl Acad Sci USA 77:1561–1565
4. Tishler RB, Schiff PB, Geard CR et al. (1992) Taxol: a novel radiation sensitizer. Int J Radiat Oncol Biol Phys 22:613–617
5. Liebmann J, Cook JA, Fisher J et al. (1994) Changes in radiation survival curve parameters in human tumor and rodent cells exposed to paclitaxel (taxol). Int J Radiat Oncol Biol phys 29:559–564
6. Gupta N, Hu LJ, Deen DF (1997) Cytotoxicity and cell-cycle effects of paclitaxel when used as a single agent in combination with ionizing radiation. Int J Radiat Oncol Biol Phys 37:885–895
7. Steren A, Sevin BU, Perras J et al. (1993) Taxol as a radiation sensitizer: a flow cytometric study. Gynecol Oncol 50:89–93
8. Rodriguez M, Sevin BU, Perras J et al. (1995) Paclitaxel: a radiation sensitizer of human cervical cancer cells. Gynecol Oncol 57:165–169
9. Milas L, Hunter NR, Mason KA et al. (1995) Tumor reoxygenation as a mechanism of taxol-induced enhancement of tumor radioresponse. Acta Oncol 34:409–412
10. Milas L, Hunter NR, Mason KA et al. (1995) Role of reoxygenation in induction of enhancement of tumor radioresponse by paclitaxel. Cancer Res 55:3564–3568
11. Schmidt-Ullrich RK, Dent P, Grant S et al. (2000) Signal transduction and cellular radiation responses. Radiat Res 153:245–257
12. Tounekti O, Kenani A, Foray N et al. (2001) The ratio of single- to double-strand DNA breaks and their absolute values determine cell death pathway. Br J Cancer 84:1272–1279
13. Vousden KH, Lu X (2002) Live or let die: the cell's response to p53. Nat Rev cancer 2:594–604
14. Ferrara N (2001) Role of vascular endothelial growth factor in regulation of physiological angiogenesis. Am J Physiol Cell Physiol 280:C1358–C1366
15. Asano M, Yukita A, Matsumoto T et al. (1995) Inhibition of tumor growth and metastasis by an immunoneutralizing monoclonal antibody to human vascular endothelial growth factor/ vascular permeability factor 121. Cancer Res 55:5296–5301
16. Gorski DH, Beckett MA, Jaskowiak NT et al. (1999) Blockage of the vascular endothelial growth factor stress response increases the antitumor effects of ionizing radiation. Cancer Res 59:3374–3378
17. Katoh O, Tauchi H, Kawaishi K et al. (1995) Expression of the vascular endothelial growth factor (VEGF) receptor gene, KDR, in hematopoietic cells and inhibitory effect of VEGF on apoptotic cell death caused by ionizing radiation. Cancer Res 55:5687–5692
18. Pidgeon G, Barr M, Harmey JH et al. (2001) Vascular endothelial growth factor (VEGF) upregulates Bcl-2 and inhibits apoptosis in human and murine mammary adenocarcinoma cells. Br J Cancer 85:273–278
19. Hovinga KE, Stalpers LJ, van Bree C et al. (2005) Radiation-enhanced vascular endothelial growth factor (VEGF) secretion in glioblastoma multiforme cell lines-a clue to radioresistance? J Neurooncol 74: 99–103
20. Dabholkar M, Vionnet J, Bostick-Bruton F et al. (1994) Messenger RNA levels of XPAC and ERCC1 in ovarian cancer tissue correlate with response to platinum-based chemotherapy. J Clin Investig 94:703–708
21. Murray D, Rosenberg E (1996) The importance of the ERCC1/ERCC4 [XPF] complex for hypoxic-cell radioresistance does not appear to derive from its participation in the nucleotide excision repair pathway. Mutat Res 364:217–226
22. Wood RD, Mitchell M, Sgouros J et al. (2001) Human DNA repair genes. Science291:1284–1289

23. You JS, Wang M, Lee SH (2003) Biochemical analysis of damage recognition process in nucleotide excision repair. J Biol Chem 278:7476–7485
24. Houtsmuller AB, Rademakers S, Nigg AL et al. (1999) Action of DNA repair endonuclease ERCC1/XPF in living cells. Science284:958–961
25. Metzger R, Leichman CG, Danenberg KD et al. (1998) ERCC1 mRNA levels complement thymidylate synthase mRNA levels in predicting response and survival for gastric cancer patients receiving combination cisplatin and fluorouracil chemotherapy. J Clin Oncol 16:309–316
26. Shirota Y, Stoehlmacher J, Brabender J et al. (2001) ERCC1 and thymidylate synthase mRNA levels predict survival for colorectal cancer patients receiving combination oxaliplatin and fluorouracil chemotherapy. J Clin Oncol 19:4298–4304
27. Lord RV, Brabender J, Gandara D et al. (2002) Low ERCC1 expression correlates with prolonged survival after cisplatin plus gemcitabine chemotherapy in non-small cell lung cancer. Clin Cancer Res 8:2286–2291
28. Warnecke-Eberz U, Metzger R, Miyazono F et al. (2004) High specificity of quantitative excision repair cross-complementing 1 messenger RNA expression for prediction of minor histopathological response to neoadjuvant radiochemotherapy in esophageal cancer. Clin Cancer Res 10:3794–3799
29. Reed E (1998) Platinum–DNA adduct, nucleotide excision repair and platinum based anti-cancer chemotherapy. Cancer Treat Rev 24: 331–344
30. Melton DW, Ketchen AM, Nunez F et al. (1998) Cells from ERCC1-deficient mice show increased genome instability and a reduced frequency of S-phase-dependent illegitimate chromosome exchange but a normal frequency of homologous recombination. J Cell Sci 111: 395–404
31. Murray D, Vallee-Lucic L, Rosenberg E et al. (2002) Sensitivity of nucleotide excision repair-deficient human cells to ionizing radiation and cyclophosphamide. Anticancer Res 22:21–26
32. Britten RA, Liu D, Tessier A et al. (2000) ERCC1 expression as a molecular marker of cisplatin resistance in human cervical tumor cells. Int J Cancer 89:453–457
33. Yacoub A, McKinstry R, Hinman D et al. (2003) Epidermal growth factor and ionizing radiation up-regulate the DNA repair genes XRCC1 and ERCC1 in DU145 and LNCaP prostate carcinoma through MAPK signaling. Radiat Res 159:439–452
34. Toiyama Y, Tanaka K, Konishi N et al. (2006) Administration sequence-dependent antitumor effects of paclitaxel and 5-fluorouracil in the human gastric cancer cell line MKN45. Cancer Chemother Pharmacol 57:368–375